Science Advances
AAAS

Supplementary Materials for

CXCL12/CXCR4-Rac1–mediated migration of osteogenic precursor cells contributes to pathological new bone formation in ankylosing spondylitis

Haowen Cui, Zihao Li, Siwen Chen, Xiang Li, Dongying Chen, Jianru Wang, Zemin Li, Wenjun Hao, Fangling Zhong, Kuibo Zhang, Zhaomin Zheng, Zhongping Zhan, Hui Liu*

*Corresponding author. Email: liuhui58@mail.sysu.edu.cn

Published 6 April 2022, *Sci. Adv.* **8**, eabl8054 (2022)
DOI: 10.1126/sciadv.abl8054

This PDF file includes:

Supplemental Figure 1

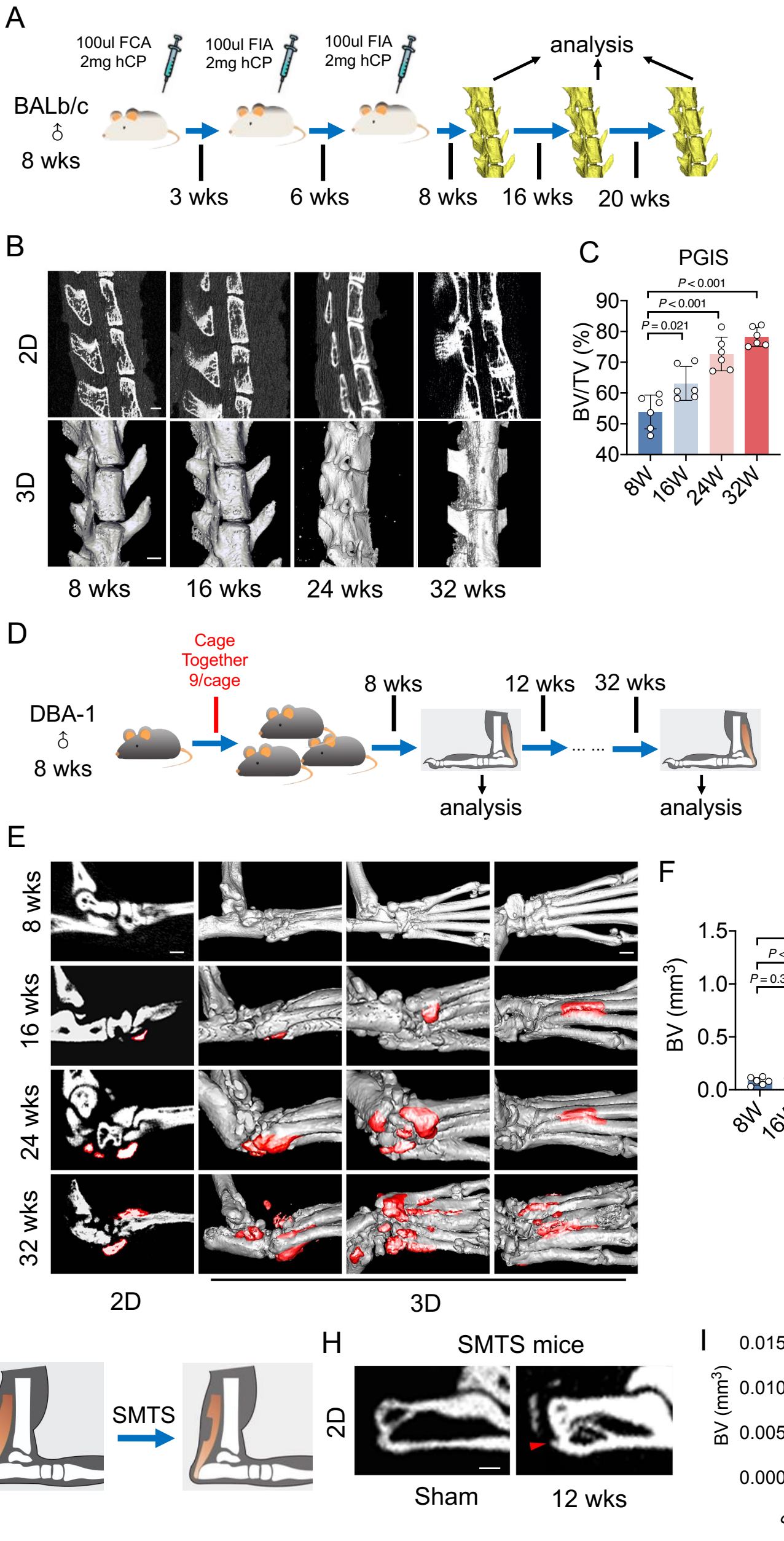

Supplemental figure 1. Establishment of three animal models for the studies of pathological new bone formation.

(A) Schematic diagram illustrating the establishment of PGIS model. (B-C) μCT images and quantitative analysis of pathological new bone formation in the spine of PGIS model. Scale bar: 500 μm. n=6 per group. ANOVA [F (3,20) =27.92] with Tukey's post hoc test was used. (D) Schematic diagram illustrating the establishment of male DBA/1 model. (E-F) μCT images and quantitative analysis of pathological new bone formation in the dorsal surface and plantar surface of hind paw of male DBA/1 model. Scale bar: 500 μm. n=6 per group. ANOVA [F(3,20) =34.52] with Tukey's post hoc test was used. (G) Schematic diagram illustrating the establishment of SMTS model. (H-I) μCT images and quantitative analysis of pathological new bone formation in SMTS model. Scale bar: 500 μm. n=6 per group. Student's t test with Shapiro-Wilk test was used. Data shown as mean ± SEM. One-way ANOVA with Levene's test, followed by the Tukey's post hoc test was used. FCA, complete Freund's adjuvant; FIA, incomplete Freund's adjuvant; hCP, human cartilage proteoglycan. SMTS; semi-Achilles tendon transection.

Supplemental Figure 2

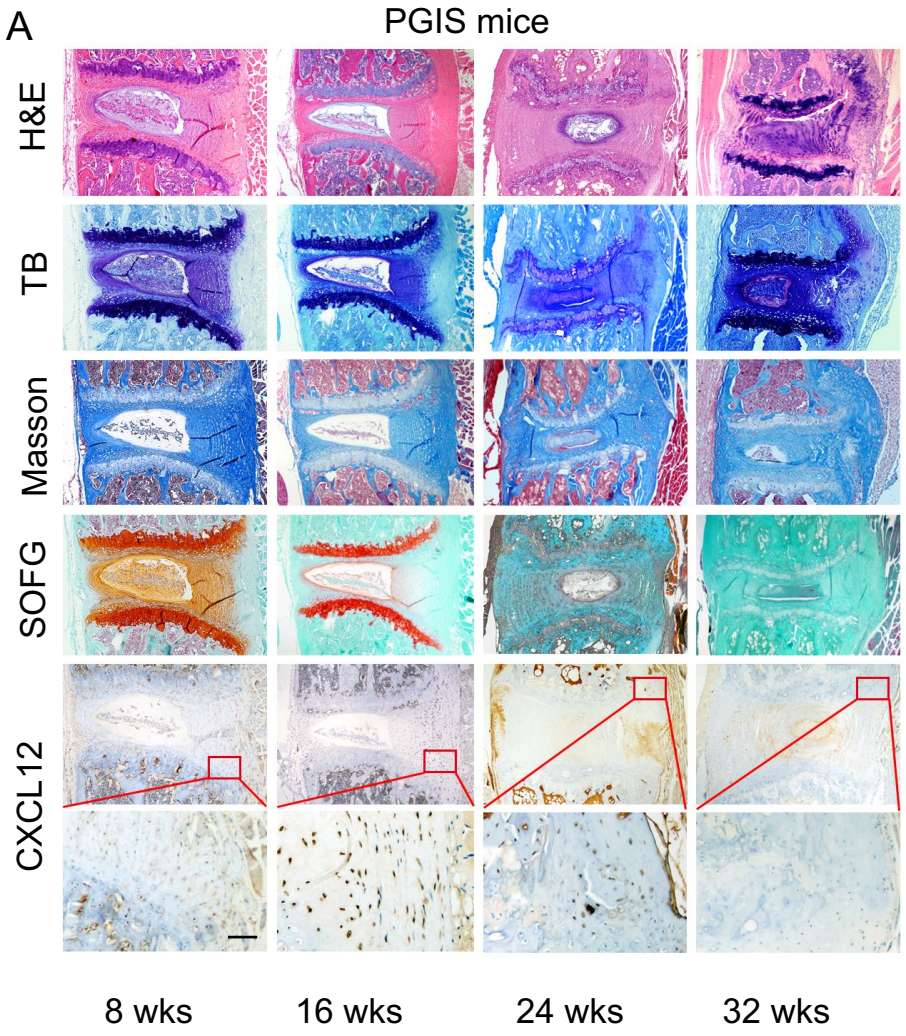

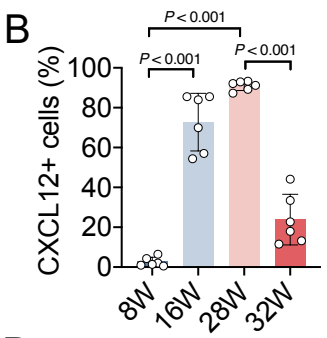

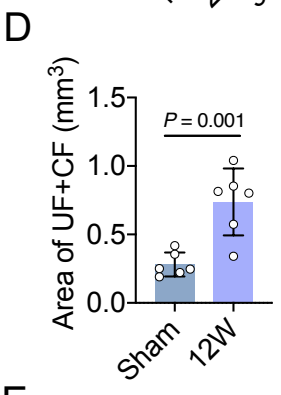

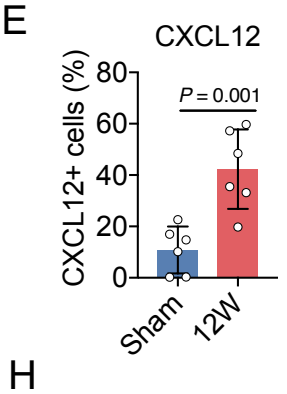

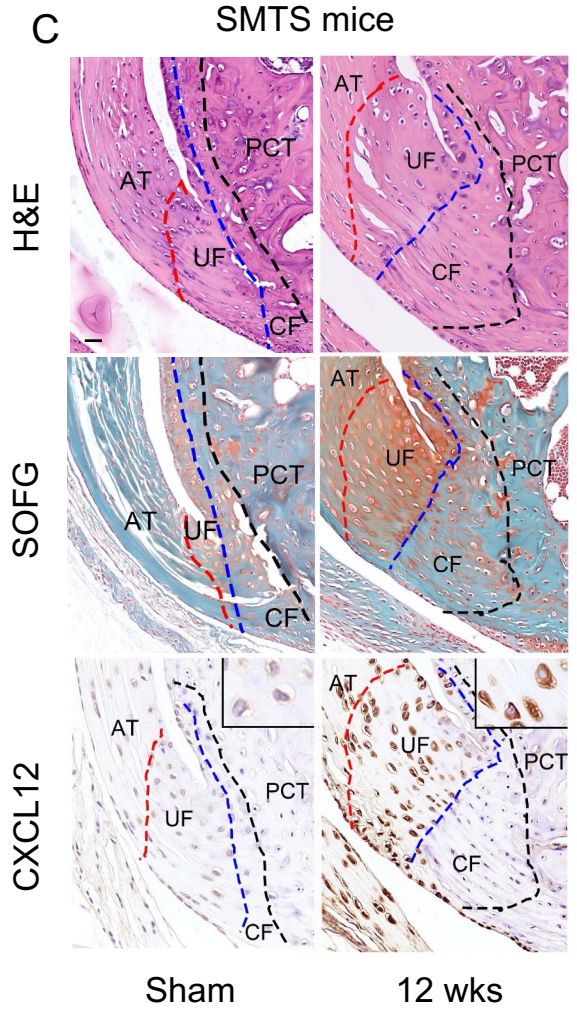

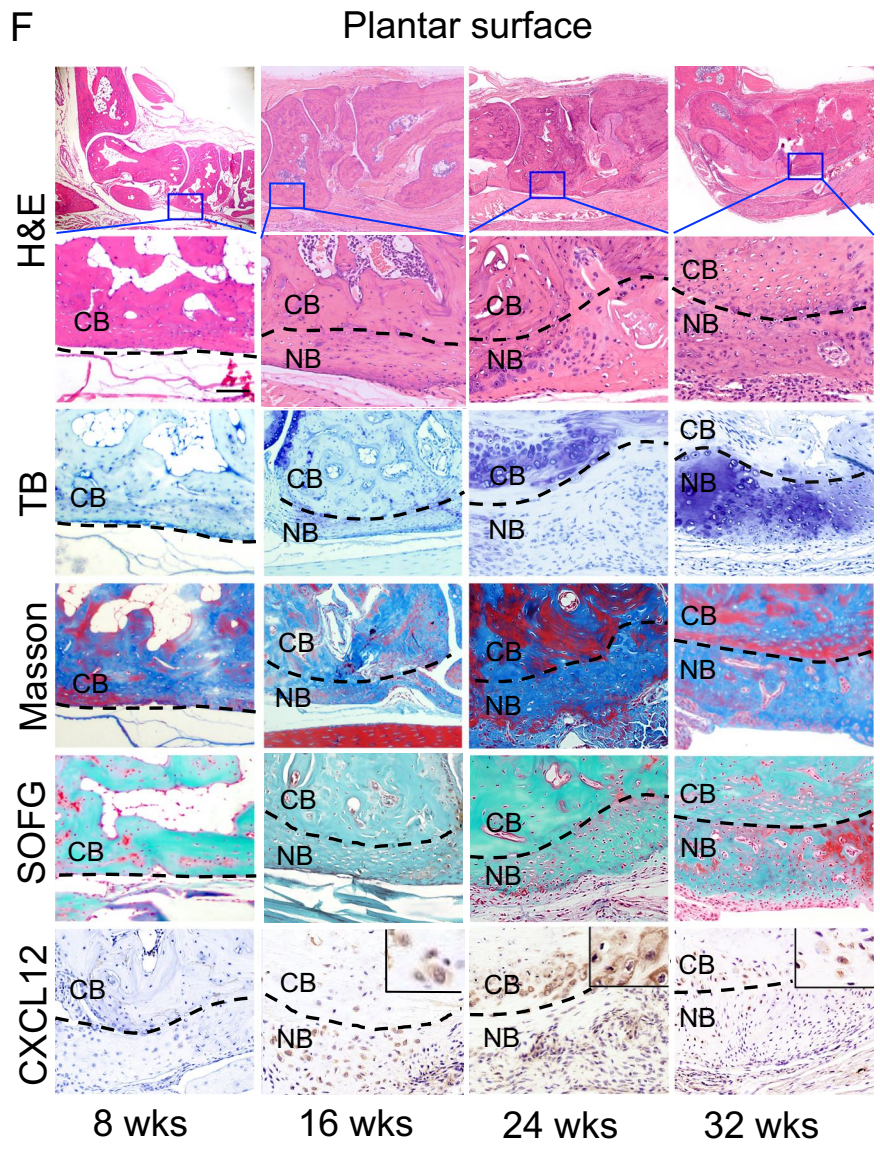

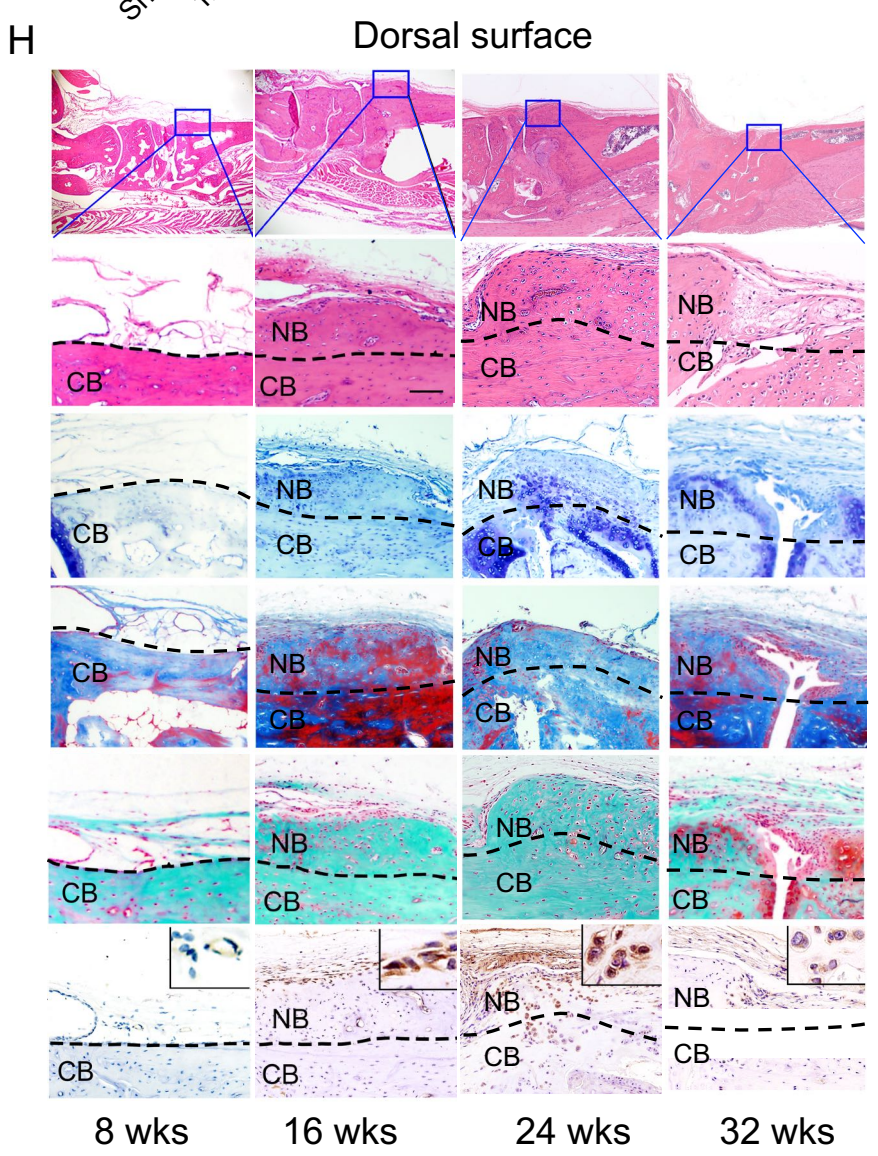

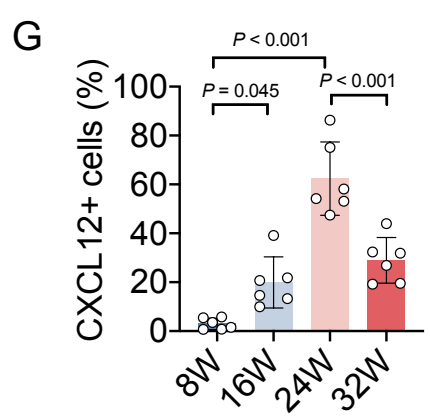

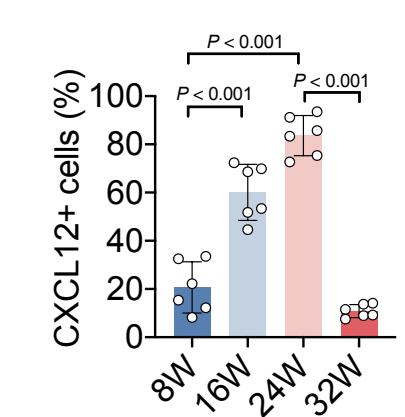

Supplemental figure 2. CXCL12 is upregulated in the ligament and entheseal tissues from animal models.

(A-B) H&E staining, TB staining, Masson staining, SOFG staining, immunohistochemical staining and quantitative analysis of CXCL12 in the spine of PGIS model. Scale bar: 200 μm. n=6 per group. ANOVA [F (3,20) =173.39] with Tukey's post hoc test was used. (C) H&E staining, SOFG staining, immunohistochemical staining of CXCL12 in SMTS model. Scale bar: 100 μm. n=6 per group. Student's t test with Shapiro-Wilk test was used. (D) Quantitative analysis of the area of uncalcified fibrocartilage and calcified fibrocartilage in (C). (E) Quantitative analysis of CXCL12 in (C). (F-G) H&E staining, TB staining, Masson staining, SOFG staining, immunohistochemical staining and quantitative analysis of CXCL12 in plantar surface of hind paw of DBA1 mice. Scale bar: 200 μm. n=6 per group. ANOVA [F (3,20) =35.17] with Tukey's post hoc test was used. (H-I) H&E staining, TB staining, Masson staining, SOFG staining, immunohistochemical staining and quantitative analysis of CXCL12 in dorsal surface of hind paw of DBA1 mice. Scale bar: 200 μm. n=6 per group. ANOVA [F (3,20) =85.14] with Tukey's post hoc test was used. Data shown as mean ± SEM. AT, Achilles tendon; UF, uncalcified fibrocartilage; CF, calcified fibrocartilage; PCT, posterior calcaneal tuberosity; CB; cortical bone; NB, new bone.

Supplemental Figure 3

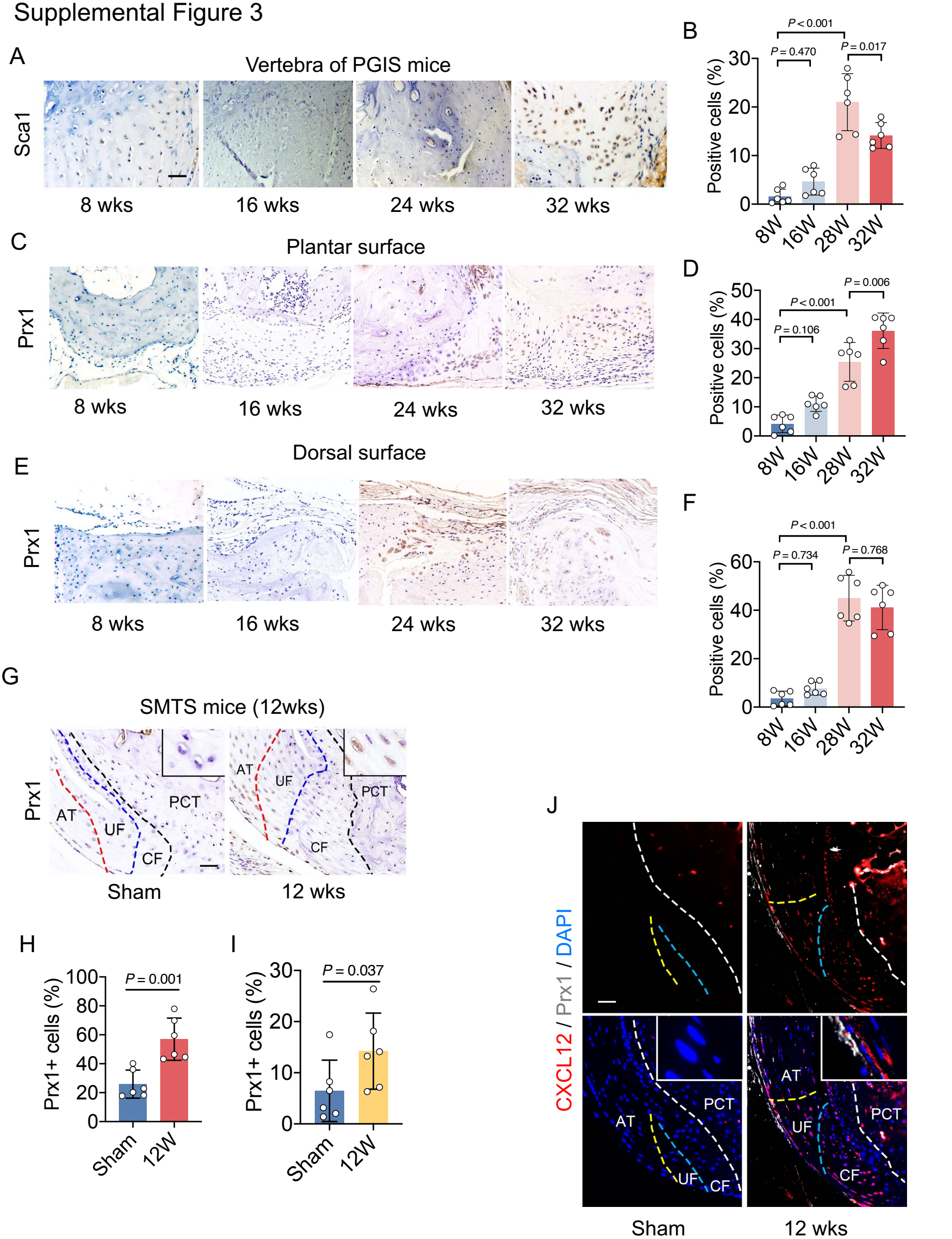

Supplemental figure 3. Osteogenic precursor cells were recruited to the sites of pathological new bone formation in animal models.

(A-B) Immunohistochemical staining and quantitative analysis of Sca1 in the spine of PGIS model. Scale bar: 50 μm. n=6 per group. ANOVA [F (3,20) =36.93] with Tukey's post hoc test was used. (C-D) Immunohistochemical staining and quantitative analysis of Prx1 in plantar surface of hind paw of DBA1 mice. Scale bar: 50 μm. n=6 per group. ANOVA [F (3,20) =50.48] with Tukey's post hoc test was used. (E-F) Immunohistochemical staining and quantitative analysis of Prx1 in dorsal surface of hind paw of DBA1 mice. Scale bar: 50 μm. n=6 per group. ANOVA [F (3,20) =59.93] with Tukey's post hoc test was used. (G-H) Immunohistochemical staining and quantitative analysis of Prx1 in SMTS model. Scale bar: 50 μm. n=6 per group. Student's t test with Shapiro-Wilk test was used. (I-J) Immunofluorescence staining and quantitative analysis of Prx1 and CXCL12 in SMTS model. Scale bar: 50 μm.Data shown as mean ± SEM. AT, Achilles tendon; UF, uncalcified fibrocartilage; CF, calcified fibrocartilage; PCT, posterior calcaneal tuberosity.

Supplemental Figure 4

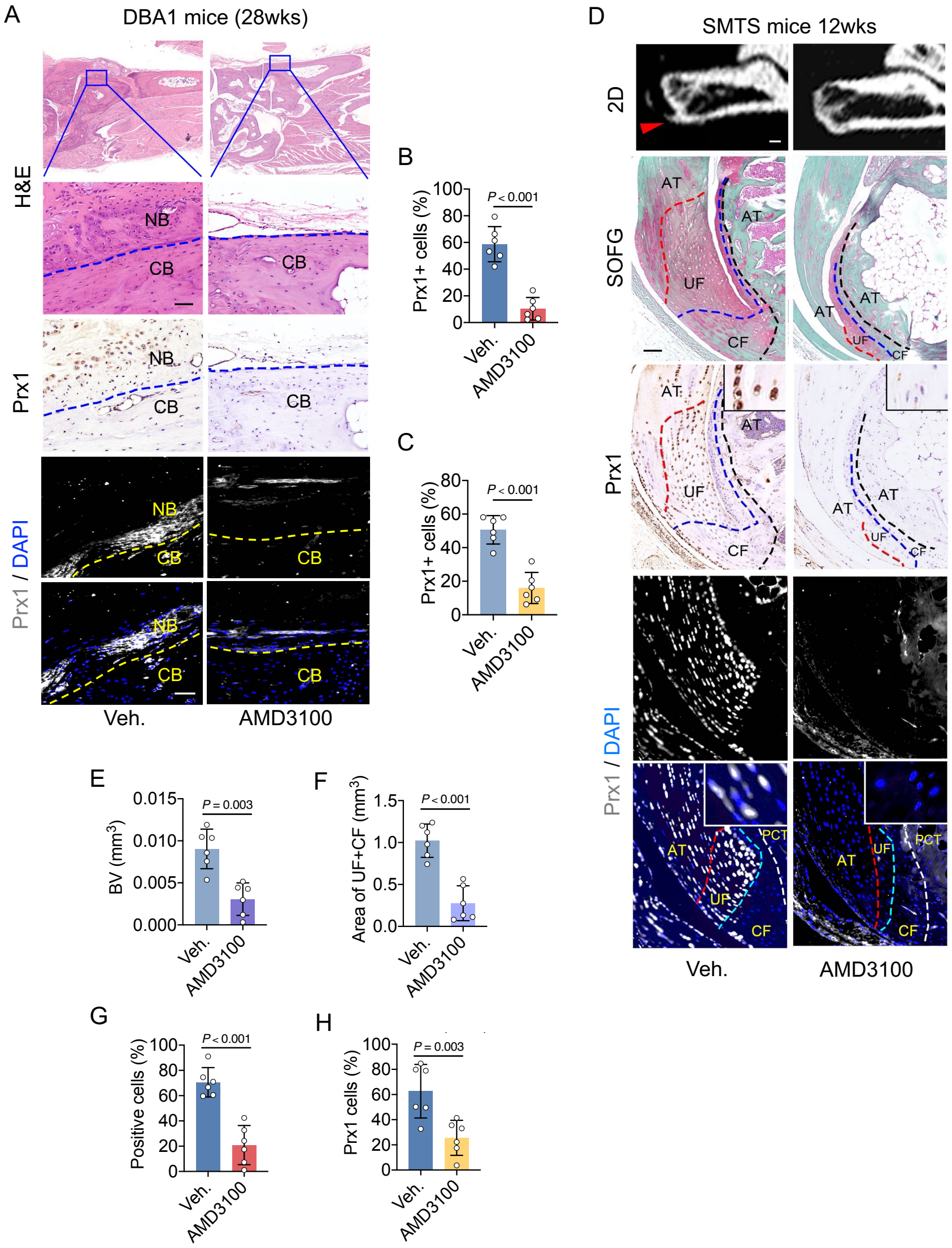

Supplemental figure 4. Inhibition of CXCL12/CXCR4 attenuates OPCs migration and pathological new bone formation.

(A-C) H&E staining, immunohistochemical staining, immunofluorescence staining and quantitative analysis of Prx1 and CXCL12 in the dorsal surface of hind paw of DBA1 mice with or without AMD3100 administration. Scale bar: 50 μm. n=6 per each group. (D) μCT images, SOFG staining, immunohistochemical staining and immunofluorescence staining of Prx1 in SMTS model. Scale bar: 50 μm. n=6 per group. (E) Quantitative analysis of pathological new bone formation in SMTS model. (F) Quantitative analysis of the area of uncalcified fibrocartilage and calcified fibrocartilage in (D). (G-H) Quantitative analysis of Prx1 in (D). Data shown as mean ± SEM. Student's t test with Shapiro-Wilk test was used. NB, new bone; CB, cortical bone; AT, Achilles tendon; UF, uncalcified fibrocartilage; CF, calcified fibrocartilage; PCT, posterior calcaneal tuberosity; AMD3100, CXCR4 inhibitor.

Supplemental Figure 5

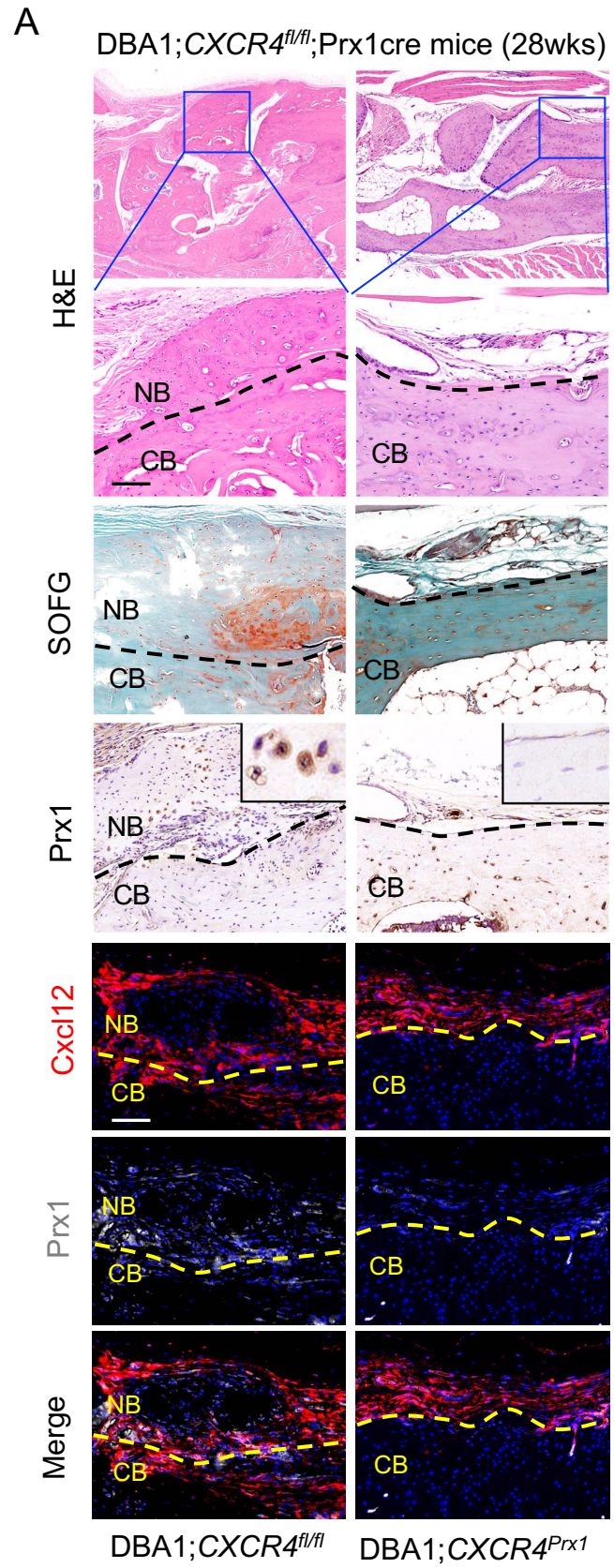

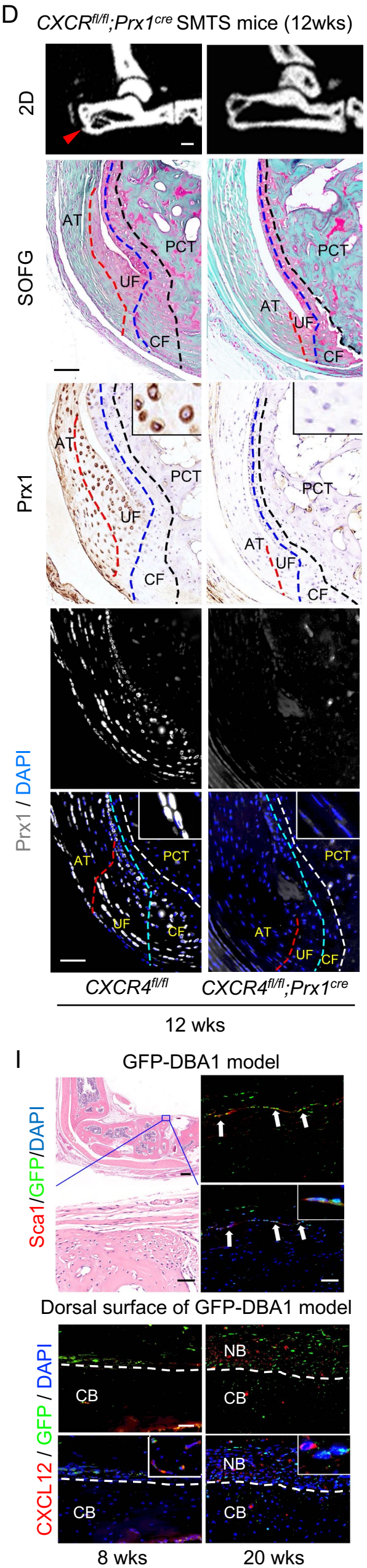

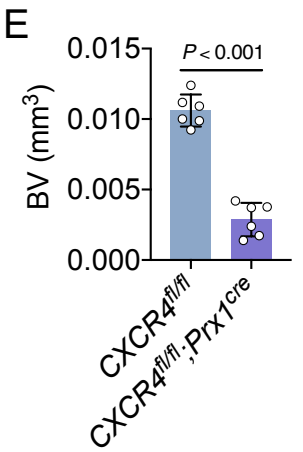

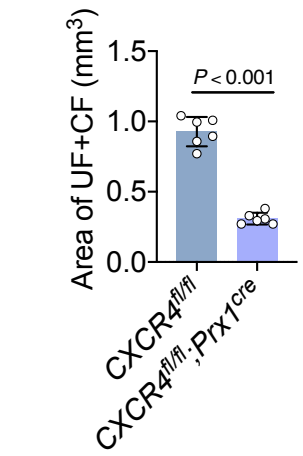

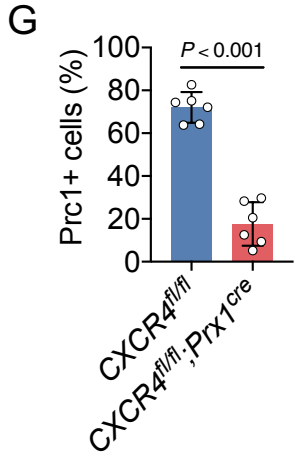

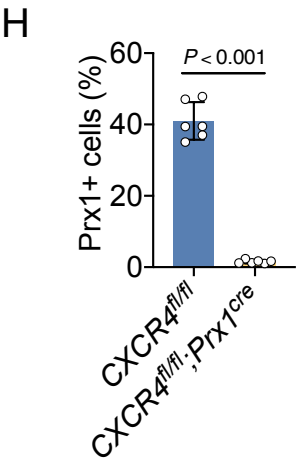

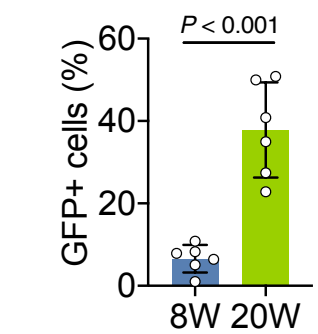

Supplemental figure 5. Conditional knockout of CXCR4 in OPCs attenuates OPCs recruitment and pathological new bone formation.

(A-C) H&E staining, SOFG staining, immunohistochemical staining, immunofluorescence staining and quantitative analysis of Prx1 in dorsal surface of hind paw of DBA/1; CXCR4$^{fl/fl}$ mice and DBA/1;CXCR4^{prx1} mice. Scale bar: 100 μm. n=6 per group. (D) μCT images, SOFG staining, immunohistochemical staining and immunofluorescence staining of Prx1 in CXCR4$^{fl/fl}$ SMTS mice and CXCR4^{prx1} SMTS mice. Scale bar: 50 μm. n=6 per group. (E) Quantitative analysis of pathological new bone formation in CXCR4$^{fl/fl}$ SMTS mice and CXCR4^{prx1} SMTS mice. (F) Quantitative analysis of the area of uncalcified fibrocartilage and calcified fibrocartilage in (D). (G-H) Quantitative analysis of Prx1 in (D). (I-J) Immunofluorescence staining and quantitative analysis of GFP and CXCL12 in the dorsal surface of hind paws of GFP-DBA1 model at the age of 8 and 20w. n=6 per group. Data shown as mean ± SEM. Student's t test with Shapiro-Wilk test was used. NB, new bone; CB, cortical bone; AT, Achilles tendon; UF, uncalcified fibrocartilage; CF, calcified fibrocartilage; PCT, posterior calcaneal tuberosity.

Supplemental Figure 6

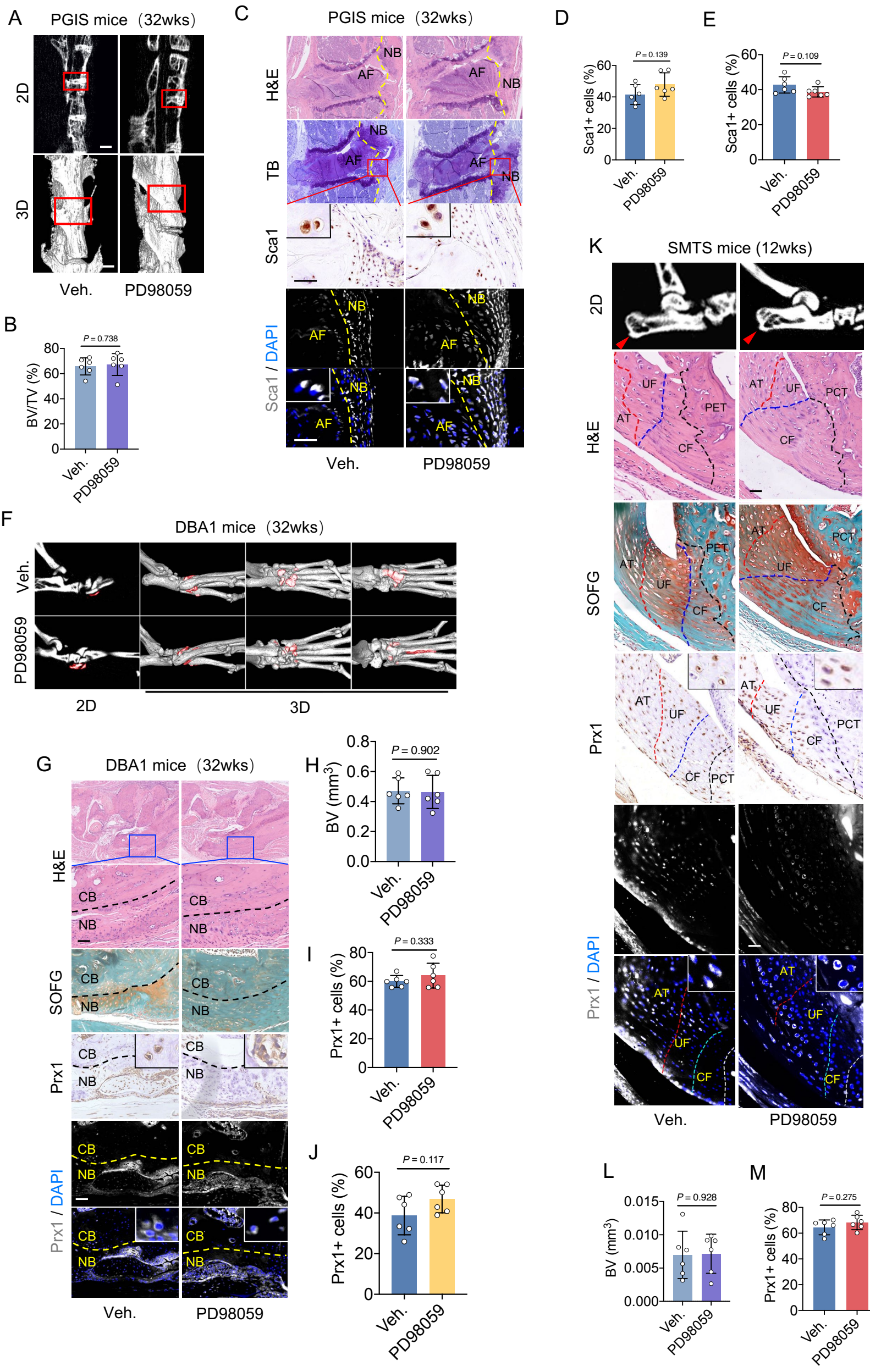

Supplemental figure 6. ERK1/2 inhibitor PD98059 had no significant suppressive effect on pathological new bone formation in animal models.

(A-B) μCT images and quantitative analysis of pathological new bone formation in PGIS mice at the age of 32w after PD98059 administration. Scale bar: 500 μm. n=6 per group. (C) H&E staining, TB staining, immunohistochemical staining and immunofluorescence staining of Sca1 in PGIS mice at the age of 32w after PD98059 administration. Scale bar: 200 μm. n=6 per h group. (D-E) Quantitative analysis of Sca1 in (C). (F) μCT images of pathological new bone formation in hind paw of male DBA/1 mice at the age of 32w after PD98059 administration. Scale bar: 500 μm. (G) H&E staining, SOFG staining, immunohistochemical staining and immunofluorescence staining of Prx1 in hind paw of male DBA/1 mice at the age of 32w after PD98059 administration. Scale bar: 200 μm. n=6 per group. (H) Quantitative analysis of pathological new bone formation in (F). (I-J) Quantitative analysis of Prx1 in (G). (K) μCT images, HE staining, SOFG staining, immunohistochemical staining and immunofluorescence staining of Prx1 in SMTS model after PD98059 administration. (L) Quantitative analysis of pathological new bone formation in SMTS model. (M) Quantitative analysis of Prx1 in (K). Data shown as mean ± SEM. Student's t test with Shapiro-Wilk test was used. NB, new bone; CB, cortical bone; AT, Achilles tendon; UF, uncalcified fibrocartilage; CF, calcified fibrocartilage; PCT, posterior calcaneal tuberosity; AF, annulus fibrosus; PD98059, ERK1/2 inhibitor.

Supplemental Figure 7

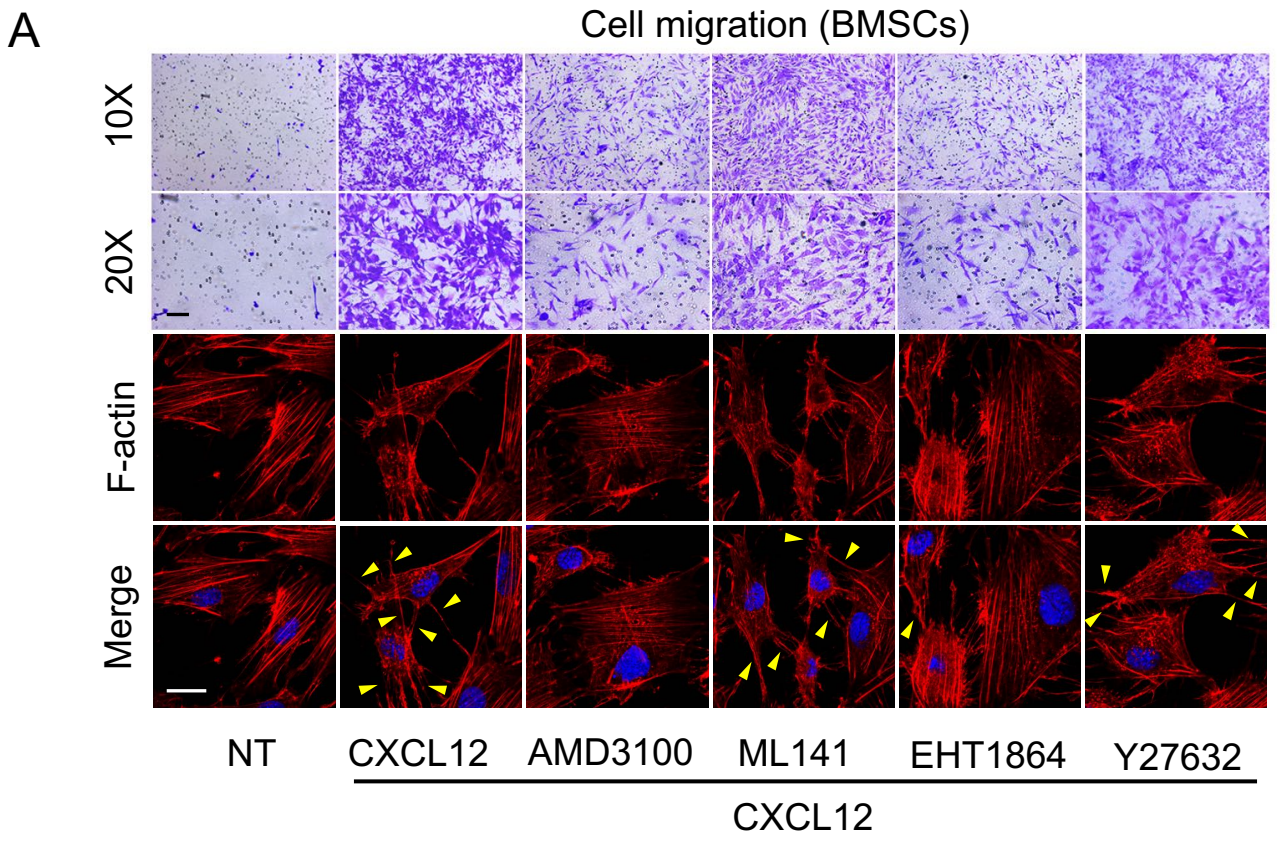

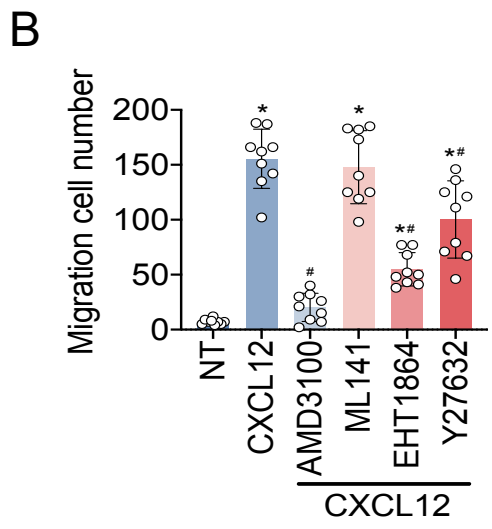

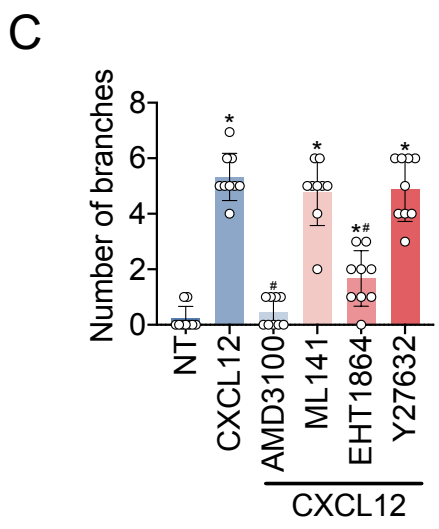

Supplemental figure 7. The CXCL12/CXCR4 axis mediates OPC migration through Rac1.

(A) Results of transwell chamber assays and immunofluorescence staining of F-actin in human BMSCs with AMD3100, EHT1864, ML141 and Y27632 administration. n=9 per group. (B) Quantitative analysis of migration cell number in (A). ANOVA [$F(5,48)=22.36$]. (C) Quantitative analysis of number of branches in (A). ANOVA [$F(5,48)=26.38$]. Data shown as mean ± SEM. *$P < 0.05$ compared with NT. #$P < 0.05$ compared with CXCL12 group by One-way ANOVA with the Bonferroni post hoc test. NT, negative control; AMD3100, CXCR4 inhibitor; ML141, cdc42 inhibitor; EHT1864, Rac1 inhibitor; Y27632, ROCK inhibitor.

Supplemental Figure 8

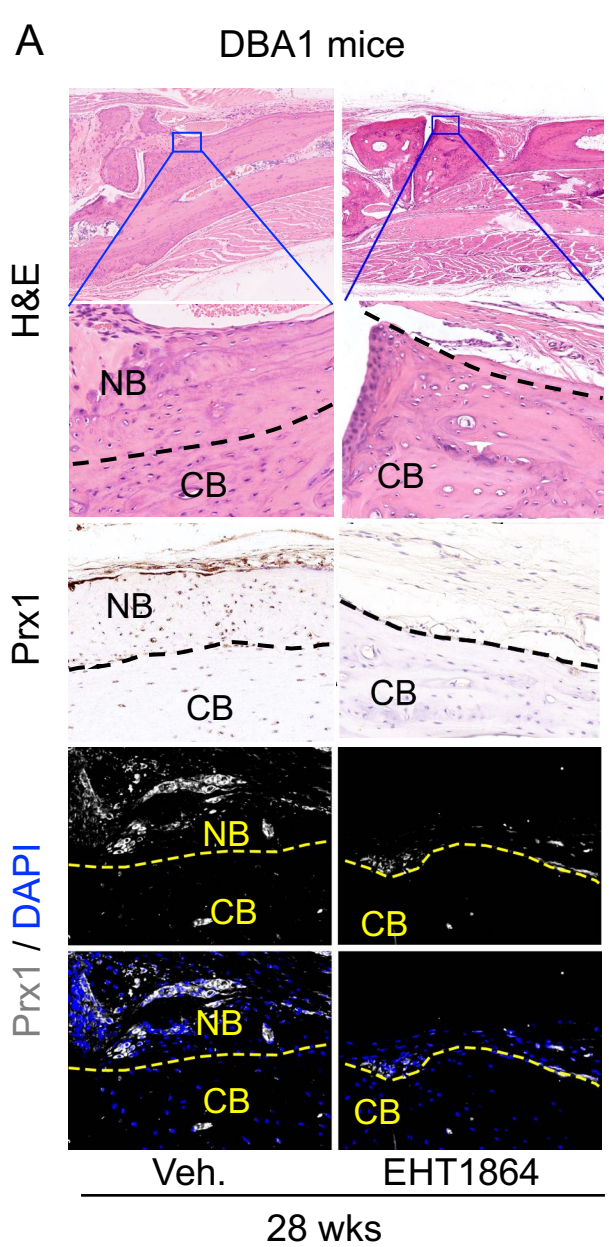

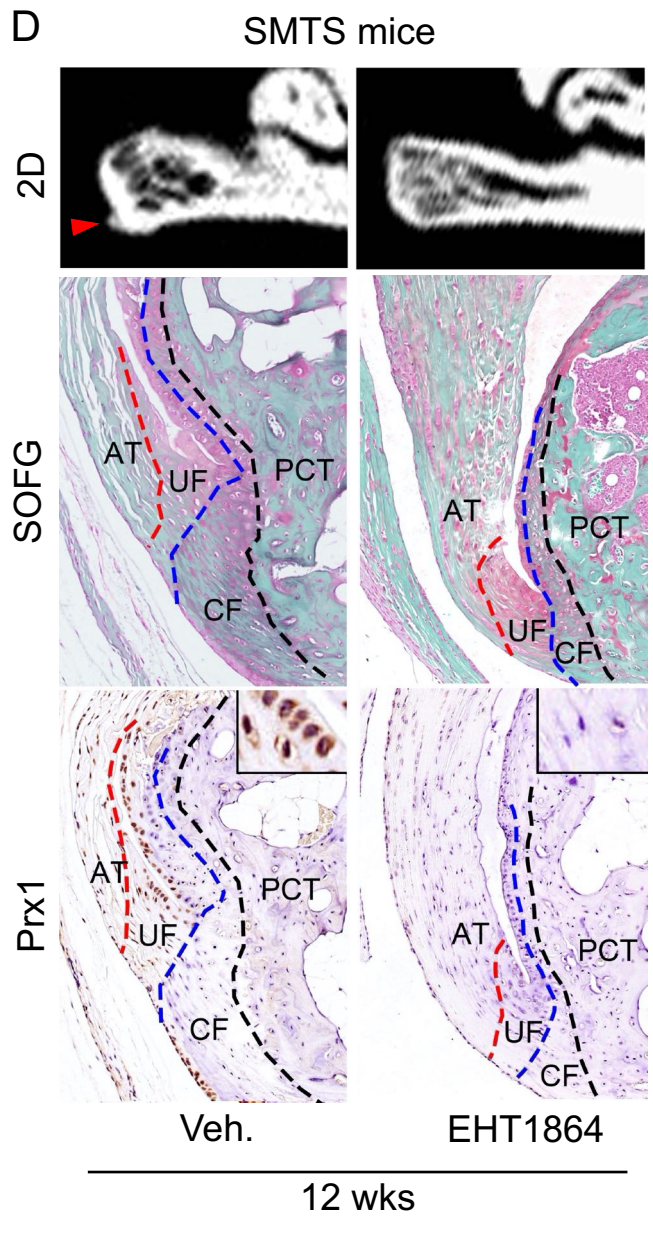

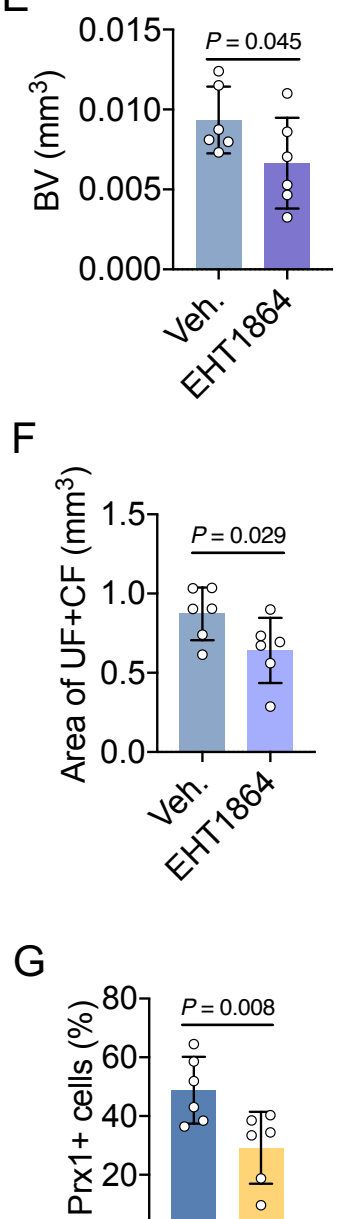

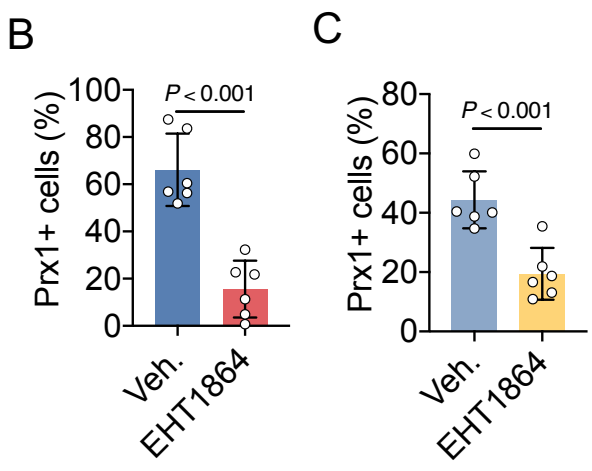

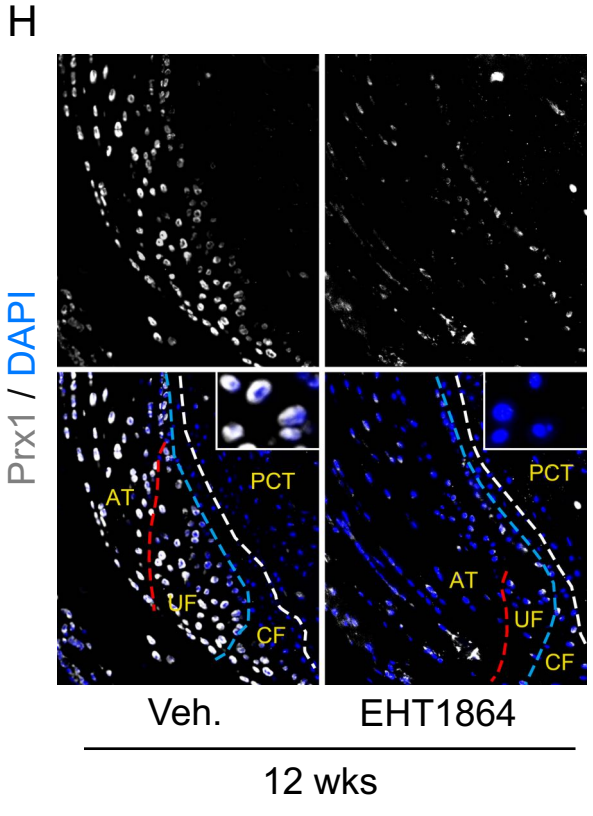

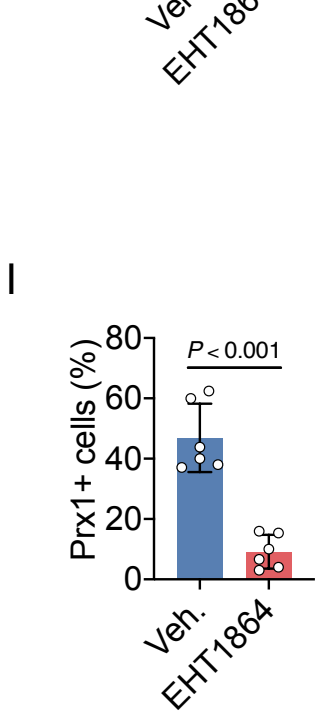

Supplemental figure 8. CXCL12/CXCR4 axis mediates OPC migration through Rac1. (A-C) H&E staining, immunohistochemical staining, immunofluorescence staining and quantitative analysis of Prx1 in dorsal surface of hind paw of DBA/1 mice with or without EHT1864 administration. Scale bar: 100 μm. n=6 per group. (D) μCT images, SOFG staining and immunohistochemical staining of Prx1 in SMTS mice with or without EHT1864 administration. Scale bar: 100 μm. n=6 per group. (E) Quantitative analysis of pathological new bone formation in SMTS mice. (F) Quantitative analysis of the area of uncalcified fibrocartilage and calcified fibrocartilage in (D). (G) Quantitative analysis of Prx1 in (D). (H-I) Immunofluorescence staining and quantitative analysis of Prx1 in SMTS mice with or without EHT1864 administration. Scale bar: 50 μm. n=6 per group. Data shown as mean ± SEM. Student's t test with Shapiro-Wilk test was used. NB, new bone; CB, cortical bone; AT, Achilles tendon; UF, uncalcified fibrocartilage; CF, calcified fibrocartilage; PCT, posterior calcaneal tuberosity; EHT1864, Rac1 inhibitor.

Supplemental Figure 9

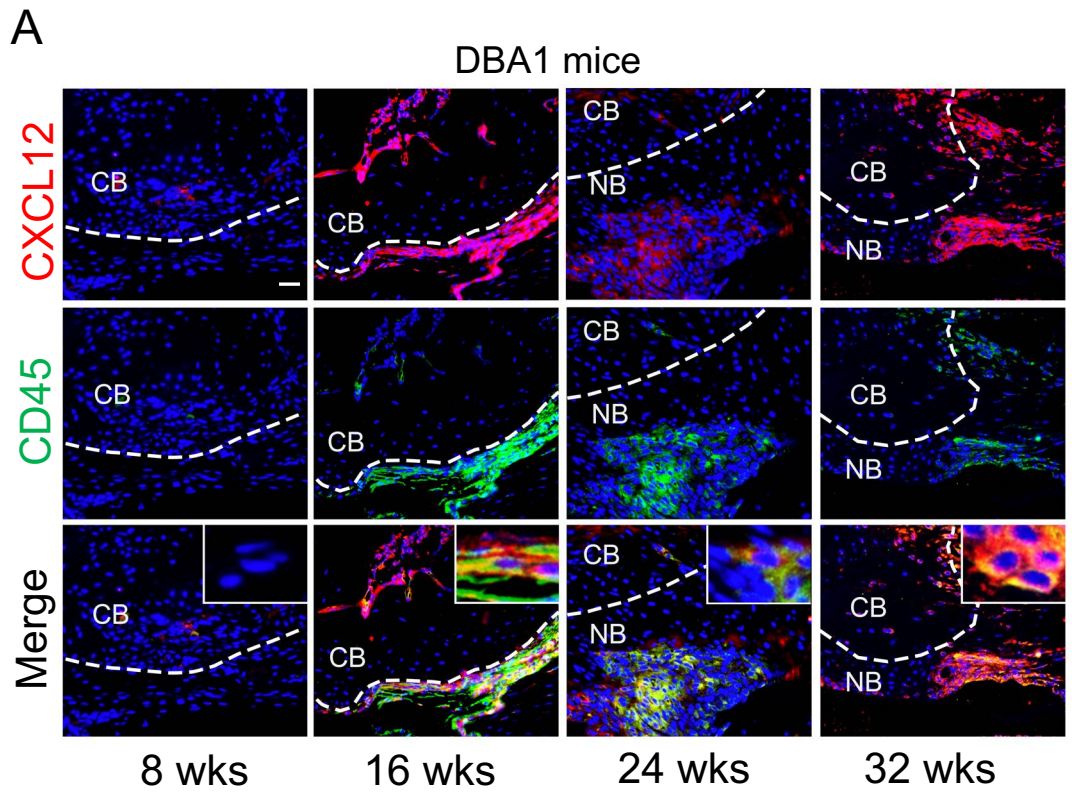

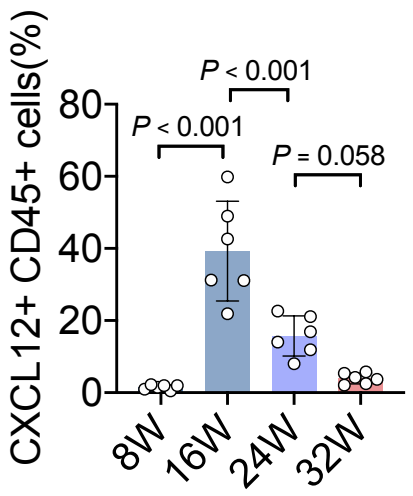

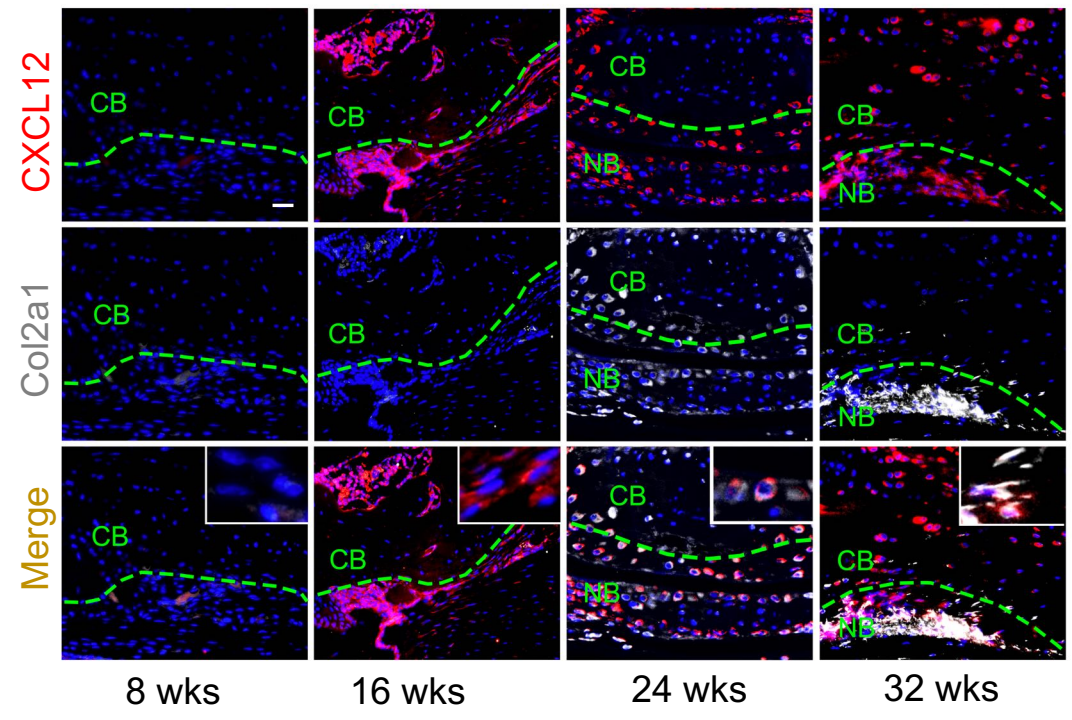

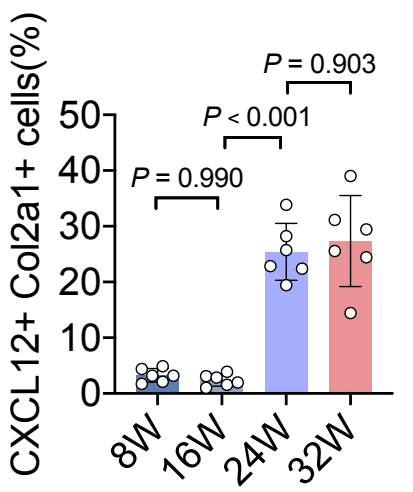

Supplemental figure 9. CXCL12 is majorly produced by CD45+ cells in the inflammatory phase and Col2a1+ cells in the endochondral ossification phase.

(A-B) Immunohistochemical staining and quantitative analysis of CXCL12 and CD45+ in male DBA/1 mice at the age of 8 ,16, 24, 32w. Scale bar: 20 μm. n=6 per group. ANOVA [F (3,20) =31.73] with Tukey's post hoc test was used. (C-D) Immunohistochemical staining and quantitative analysis of CXCL12 and Col2a1 in male DBA/1 mice at the age of 8 ,16, 24, 32w. Scale bar: 20 μm. n=6 per group. ANOVA [F (3,20) =46.62] with Tukey's post hoc test was used. Data shown as mean ± SEM. NB, new bone; CB, cortical bone.

Supplemental Figure 10

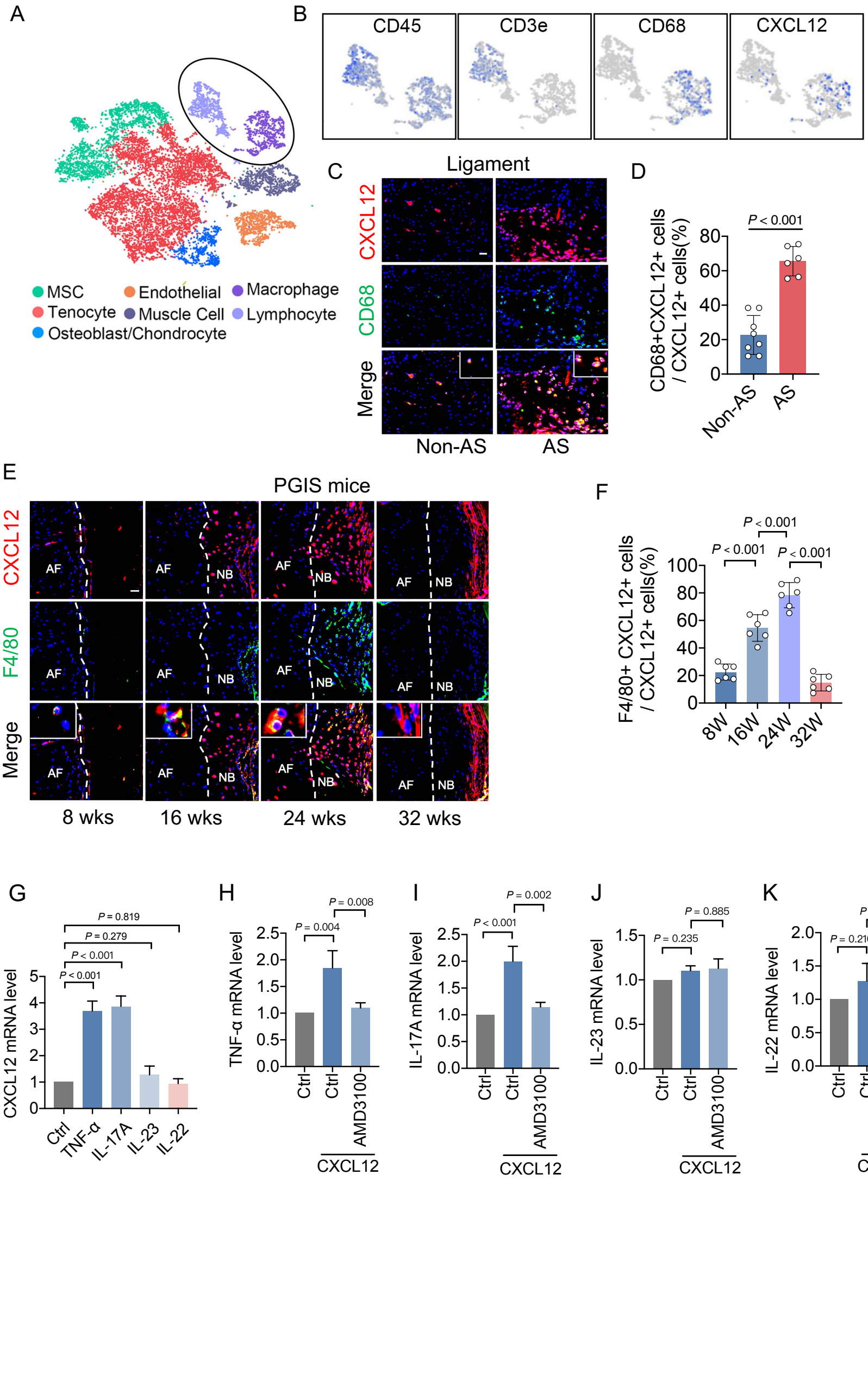

Supplemental figure 10. Inflammatory cytokines induced CXCL12 overexpression in a feedforward manner.

(A) 2-dimensional space through t-stochastic neighbor embedding (t-SNE) analysis of single-cell RNA sequencing from spinal entheseal tissuses revealed 7 distinct cell clusters. (B) Feature plots displaying the expression of CD45, CD3e, cd68 and CXCL12. (C-D) Immunohistochemical staining and quantitative analysis of CXCL12 and CD68 in spinal ligament tissues of AS and non-AS patients. Scale bar: 20 μm. n = 6 tissues from AS patients VS n=8 tissues from non-AS patients. Student's t test with Shapiro-Wilk test was used. (E-F) Immunohistochemical staining and quantitative analysis of CXCL12 and F4/80 in PGIS mice at the age of 8 ,16, 24, 32w. Scale bar: 20 μm. n=6 per group. ANOVA [F (3,20) =33.89] with Tukey's post hoc test was used. (G) RT-qPCR analysis of expression of CXCL12. ANOVA [F (4,10) =76.06] with the Bonferroni post hoc test was used. (H-K) RT-qPCR analysis of expression of TNF-α (ANOVA [F (2,6) =16.76]), IL-17A (ANOVA [F (2,6) =30.38]), IL-23 (ANOVA [F (2,6) =3.00]) and IL-22 (ANOVA [F (2,6) =2.00]). One-way ANOVA with the Bonferroni post hoc test was used. Data shown as mean ± SD.

Supplemental Figure 11

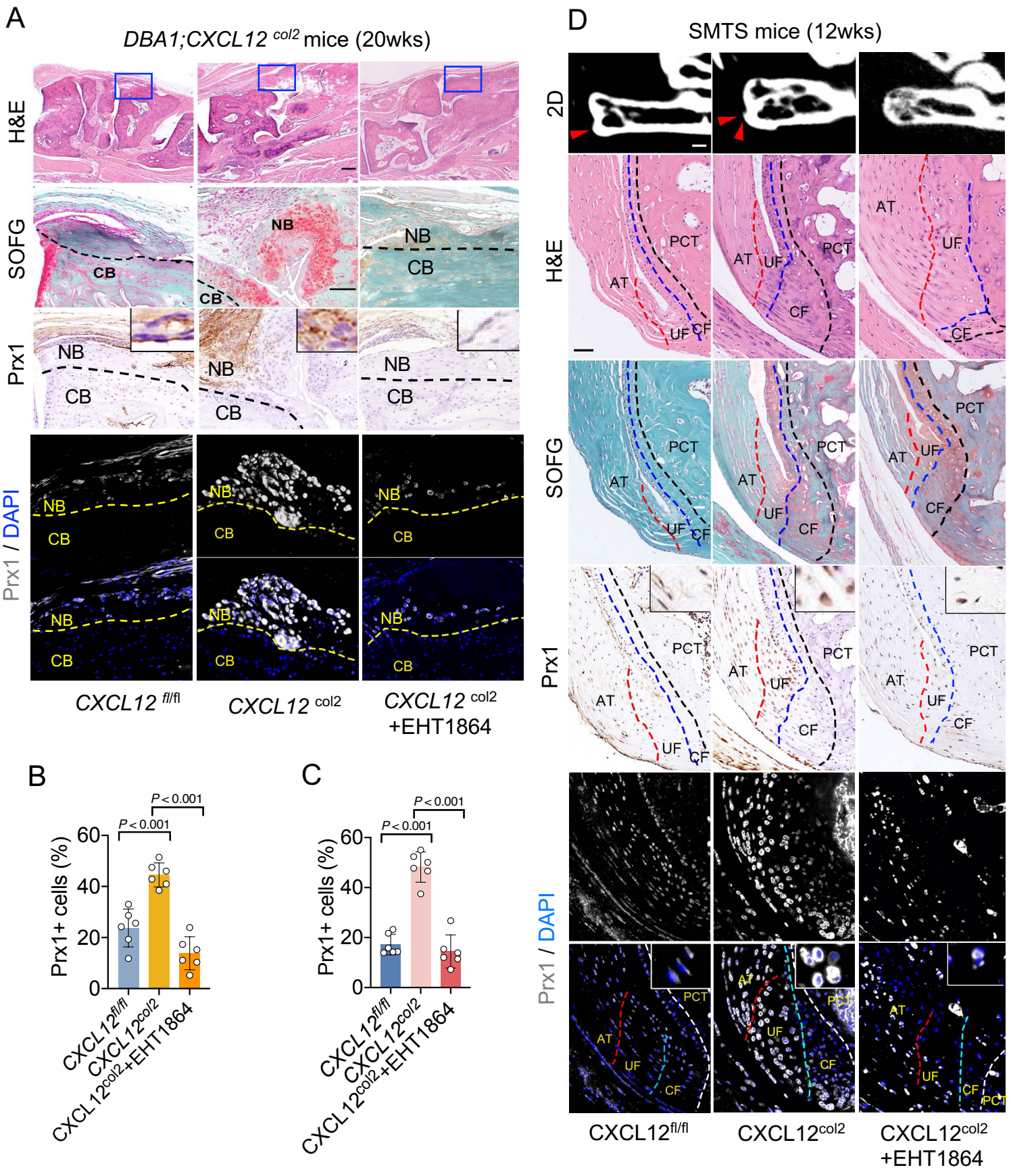

Supplemental figure 11. DBA1;CXCL12$^{Col2\text{-}cre}$ mice develops an ankylosis phenotype. (A) H&E staining, SOFG staining, immunohistochemical staining and immunofluorescence staining of Prx1 in dorsal surface of hind paw of DBA1;CXCL12^{Col2} mice at the age of 20w with or without EHT1864 administration. Scale bar: 200 μm. n=6 per group. (B-C) Quantitative analysis of Prx1 in (A). ANOVA [F(2,15) =37.06; F(2,15) =63.72] with Tukey's post hoc test was used. (D) μCT images, HE staining, SOFG staining and immunohistochemical staining and immunohistochemical staining of Prx1 in CXCL12^{Col2} SMTS mice with or without EHT1864 administration. (E) Quantitative analysis of pathological new bone formation in CXCL12^{Col2} SMTS mice with or without EHT1864 administration. n=6 per group. ANOVA [F(3,20) =12.56] with Tukey's post hoc test was used. (F-G) Quantitative analysis of Prx1 in (D). n=6 per group. ANOVA [F (2,15) =45.86; F (2,15) =37.06] with Tukey's post hoc test was used. Data shown as mean ± SEM. NB, new bone; CB, cortical bone; AT, Achilles tendon; UF, uncalcified fibrocartilage; CF, calcified fibrocartilage; PCT, posterior calcaneal tuberosity; EHT1864, Rac1 inhibitor.

Supplementary table 1. Demographic and clinical data of patients.

Table S1. Demographic and clinical data of patients

	Non-AS n=8	AS n=6
Sample	bone ligamentum flavum supraspinatus ligament interspinous ligament	bone ligamentum flavum supraspinatus ligament interspinous ligament
Age	31.75±9.71	36.83±7.57
Sex(M/F)	5/3	6/0
BASDAI	/	5.08±1.20
BASFI	/	6.00±0.88
HLA-B27(+/-)	0/8	6/0
Treatment before surgery	NSAIDs	NSAIDs DMARD
Main diagnosis	Idiopathic Scoliosis	AS
Surgical indication	Severe Scoliosis Neurological Compression	Severe Kyphosis

AS: Ankylosing Spondylitis, BASDAI: Bath Ankylosing Spondylitis Disease Activity Index. BASFI: Bath Ankylosing Spondylitis Functional Index.

Supplementary table 2. Demographic and clinical data of patients from whom blood samples were collected.

Table S2. Demographic and clinical data of patients

	Non- Ankylosing Spondyliyis n=27	Non radiographic axial spondylosrthritis n=23	Ankylosing Spondyliyis n=22
Sample	serum (2ml)	serum (2ml)	serum (2ml)
Age	28.96±20.84	32.87±12.93	37.73±10.06
Sex(M/F)	10/17	17/6	19/2
BASDAI	/	2.30±0.61	4.68±1.08
BASFI	/	3.23±0.97	5.44±0.96
Treatment	/	NSAIDs DMARD	NSAIDs DMARD

AS: Ankylosing Spondylitis, SpA: Spondyloarthritis, BASDAI: Bath Ankylosing Spondylitis Disease Activity Index. BASFI: Bath Ankylosing Spondylitis Functional Index.